# Vibrational density of states in the archetypical icosahedral quasicrystal $i$-Al$_{62}$Cu$_{25.5}$Fe$_{12.5}$: Neutron time-of-flight results

R. A. Brand*

*Department of Physics, Gerhard-Mercator-Universität Duisburg, D-47048 Duisburg, Germany*

A.-J. Dianoux

*Institute Laue-Langevin, BP 156, F-38043 Grenoble CEDEX-9, France*

Y. Calvayrac

*CECM/CNRS, 15, rue G. Urbain, F-94407 Vitry CEDEX, France*

(Received 27 March 2000)

We study the neutron-weighted vibrational density of states $g(E)$ in the $i$-AlCuFe quasicrystal measured by time-of-flight inelastic neutron scattering (INS). The samples studied were $i$-Al$_{62}$Cu$_{25.5}$Fe$_{12.5}$ with different isotopic substitutions. These results are compared to our previous $^{57}$Fe inelastic nuclear-resonant absorption (INA) results for the iron-partial $g(E)$ [R. A. Brand *et al.*, Phys. Rev. B **59**, R14 145 (1999)]. The neutron-weighted $g(E)$ measured on samples with different isotopes (natural Cu and $^{65}$Cu; natural Fe and $^{57}$Fe) shows that the aluminum and copper-partial $g(E)$ is strongly peaked at a significantly lower energy than that for iron. We show in addition that the low-energy square term in $g(E)$ is the same for both INS and INA but a significant *quartic term* exists in the neutron-weighted $g(E)$. The neutron-weighted and iron-partial $g(E)$ are used to calculate lattice-dynamical properties such as the lattice specific heat $C_{\text{latt}}(T)$. The $C_{\text{latt}}(T)$ as calculated from the neutron-weighted $g(E)$ agrees with the experimental $C_{\text{latt}}$ in the low $T$ range where an anomalous power law had previously been found [J. C. Lasjaunias *et al.*, J. Phys. I **7**, 959 (1997)]. These results are discussed in terms of possible non-acoustic modes at low energy.

## I. INTRODUCTION

### A. Lattice dynamics of quasicrystals

The discovery of quasicrystalline alloys with icosahedral ($i$-) point symmetry[1] profoundly changed conventional crystallography. In addition, this interesting type of long-range nonperiodic order has led to different dynamical properties in these materials. Theoretical considerations show that there are two types of elementary excitations of the lattice degrees of freedom: phonons and phasons.[2] The vibrational density of states (VDOS) $g(E)$ predicted from many models[3–6] is highly structured at high energy, with an infinite number of van Hove singularities. However in the low-energy limit, the weight of these singularities diminishes so that well defined acoustic modes are expected. The VDOS is thus predicted to be Debye-like (quadratic in $\omega$ or $E$) at low energy in these calculations.[3–5] The character of the vibrational eigenstates in an aperiodic lattice depends on the competition between two characteristic features. The first is the aperiodicity, which leads to a tendency for localization. The second is the the self-similarity which means that any finite section will be repeated infinitely many times. This leads to a tendency for extended states. Numerical studies[7] have shown that most states are ''critical'': they are intermediate between extended and localized and show power-law decay.

Many types of techniques have been applied to the study of phonon dynamics $i$-AlCuFe and QC in general. Coherent inelastic neutron scattering (INS) has been used to study the phonon dispersion relations $\omega(\vec{k})$ in $i$-AlPdMn,[8,9] in $i$-AlLiCu,[10,11] and in $i$-AlCuFe.[12,13] Generally well-defined

acoustic phonon modes with instrumental linewidth are found below a certain wave vector $\vec{k}$ of about 0.4 Å$^{-1}$. Above this, they broaden out into a band of mixed acoustic and optical modes.[8,9] However, it has been shown that the expected proportionality between the dynamical and the static structure factor holds, so that the acoustic branches are seen in coherent INS.[5] It is not possible strictly speaking to define a Brillouin zone for a quasiperiodic lattice. But one result from the elastic and inelastic scattering studies is that it is possible to define a pseudo-Brillouin zone (PBZ) defined from the strongest diffraction peaks.[5]

On the other hand, inelastic neutron-scattering measurements lead to smooth featureless ''generalized'' vibrational density of states (GVDOS).[14–16] In the case of $i$-AlCuFe this is a smooth VDOS with double maximum. The GVDOS has been studied in $i$-AlPdMn at higher temperatures:[16] a general softening is found which correlates with the high-temperature transition to soft plasticity. As we shall see, a major problem with studies of the VDOS using incoherent inelastic nuclear scattering is the difficulty of removing (at least approximately) the multiphonon contributions. In, for example, Refs. 14, multiphonon corrections could only be calculated assuming a uniform effective mass over the energy range (see, for example, Ref. 17, Chap. 7.6). As we shall see later, this initial simplest model (justified at the time) is not sufficient to correctly account for the heterogeneous structure of the effective mass as can be seen from the iron-partial VDOS presented in Ref. 18.

Several systems have also been studied by specific heat[19–22] and thermal conductivity, ultrasound, and light scattering.[5] In the case of $i$-AlPdMn, the usual expression,

$$C_V = \gamma T + \beta T^3 + \delta T^5, \qquad (1)$$

has been used by Wälti et al.[22] and Chernikov et al.[19] to explain the measured low-temperature specific heat. As usual, the first term, $\gamma T$, is due to the conduction electrons, where the value of $\gamma$ is reduced as compared to similar metals, reflecting the low density of electronic states at the Fermi energy. The latter two terms are the lattice contributions $C_{\text{latt}}$. A Debye-like phonon density of states would lead to the $\beta T^3$ term alone (equivalent to a linear dispersion relation $\omega = v|\vec{k}|$). Wälti et al.[22] have also discussed the disagreements between different physical properties testing the initial Debye-like part of the VDOS. They compared the phonon $T^3$ term in $C_{\text{latt}}$ with that predicted from the measured speed of sound, and with that predicted from the measured neutron-weighted GVDOS. The strong disagreement with the predictions based on the GVDOS might be traceable to experimental problems with the inelastic neutron-scattering result (difficulty of multiphonon corrections in the GVDOS, problems with removing the elastic peak from the small energy region: see Ref. 22). However, they did note that the measured sound velocity would predict a smaller cubic term than that derived from specific-heat data. This can be attributed to nonacoustic vibrations at low energy. One difficulty with the specific heat of $i$-AlPdMn is the presence of a low-temperature magnetic transition, making the extraction of the lattice specific heat itself rather difficult.[23–25] The low-temperature variation of the sound velocity has been interpreted in terms of the existence of nonacoustic low-energy tunnel states in $i$-AlCuFe,[26] $i$-AlPdMn,[27] and $i$-MgZnY.[28]

Equivalent to calculating the $T^3$ term in $C_{\text{latt}}$, we can compare different physical properties which measure lattice vibrations through the calculated Debye temperature $\Theta_D$ (as we do in the following). In the Debye model, the Debye temperature enters various different experimental parameters such as the lattice specific heat $C_{\text{latt}}$, the Debye-Waller factor in both diffraction and in EXAFS, the average (Debye) speed of sound $v_D$, and the vibrational density of states $g(E)$. The values of $\Theta_D$ calculated from most of these different parameters are not the same since the physical parameters are sensitive to different energy regions of $g(E)$ [usually as a power of the energy $E$ in an integral over $g(E)$]. We present values of $\Theta_D$ both as calculated by using the initial curvature of $g(E)$ at small $E$ and by averaging $g(E)$ over $E$. We emphasize that the first method is essentially in the zero energy, zero wave-vector limit and thus usually tests the long wavelength acoustic phonons. We will compare these with values of $\Theta_D$ determined from the speed of sound, as well as the measured low-temperature lattice specific heat from Lasjaunias et al.[21] In crystalline materials these different calculations generally agree well (see Ref. 29, Chap. 2 for a discussion, and Ref. 30 for a recent work on metallic iron). We present our results as well in terms of an effective Debye cutoff energy as defined for a pure Debye model, or including the first corrections (quartic term in energy).

In nonmetallic amorphous materials,[31] large discrepancies between the predictions of the sound velocity, and the specific heat below 1–2 K are well known. The specific heat varies linearly with $T$ (although the system is insulating), instead of the expected $T^3$ from the Debye model, and is much larger than that expected from the speed of sound.

Thus there must be additional excitations of the lattice degrees of freedom (often described as two level systems, TLS, also denoted tunneling states[32,33]). At higher temperatures, these additional states are often described in terms of the "soft potential model."[34] A broad band of excitations is postulated in this model, extending from the low-energy tunneling states (TLS) up to localized harmonic excitations at higher energies. Many computer simulations[35] have also shown these vibrational modes in simple models. Although this model has recently been questioned,[36] it has been successfully used to describe the thermal and vibrational properties of glasses. One aspect of these studies interesting for the current study is the realization that these local TLS can be due to the motion of groups of atoms in a collective manner,[37] as well as that they can interact with the extended sound wave states.[38] We return to this point later when we discuss possible models for the lattice dynamics in quasicrystals.

The specific heat of icosahedral $i$-Al$_{62}$Cu$_{25.5}$Fe$_{12.5}$ has been studied by Lasjaunias et al.[21] Their results seem to indicate a complicated behavior for the lattice contribution $C_{\text{latt}}$ in the low-temperature region with nonintegral power expression $T^{3.55}$ being used by the authors to describe their results. These results were, however, difficult to understand since the lattice thermal properties of $i$-AlCuFe are not expected to be different from those of the other icosahedral quasicrystals. We will address this point by calculating the lattice specific heat directly from the measured vibrational density of states in the case of $i$-AlCuFe, and comparing this to the results presented by Lasjaunias et al.[21]

We will discuss the different lattice-dynamical behavior of iron and copper presented here in terms of the local configuration around the iron and copper atomic sites. In order to do this, we present a short description of the perfect icosahedral quasicrystal model. The structure of the stable quasicrystalline phases (such as $i$-AlCuFe and $i$-AlPdMn) is best described by this model.[39] The six-dimensional (6D) face-centered Bravais lattice is decorated by three different atomic surfaces[40] denoted "node" $n$, "node-prime" $n'$ and "body-center" $bc$. The problem of the atomic decoration is the most difficult, and only partially resolved. The proposed atomic decoration[39,41] consists of Al and Fe on $n$, Cu on $bc$, and all three on $n'$ atomic surfaces. The atomic structure is then obtained by projection into the 3D parallel space. It turns out that much of the resulting structure can be described very simply. The Cu $bc$ sites are surrounded by 12 Al $n$-site atoms on an icosahedron, and 20 Al, Cu, and Fe $n'$-site atoms on a dodecahedron. This forms a cluster of 33 atoms reminiscent of the Bergman cluster, and about 65% of the structure can be thus described. The remaining ca. 35% of the structure is built from pieces of what seem to be Mackay icosahedra. It is known that the icosahedral phase is stable in the AlCuFe ternary system along a line of composition, rather than at one point.[42] It is the Makay icosahedra which provide the chemical flexibility necessary to explain this property. For both Cu and Fe, the nearest-neighbor shell is dominated by Al. From this model, it is quite clear that iron and copper play a very different role in the structure, and this is the origin of the different lattice dynamics which will be presented here. Characteristic is the absence of Fe on $bc$ sites occupied by Cu. These structural differences be-

tween the lattice sites occupied by Cu and Fe will justify a simple model for the effective vibrating mass in different energy regions of $g(E)$. It is also interesting to note the large differences in the phason dynamics between Cu and Fe which have been found by quasielastic scattering experiments as well.[43,44]

### B. Inelastic methods: Vibrational density of states

In addition to INS, a different method to study the vibrational density of states is provided by inelastic nuclear-resonant absorption (INA) of synchrotron radiation, reviewed in Ref. 45. This method yields the element-partial $g(E)$ directly. Recently[18] we have addressed the question of the phonon structure in quasicrystals using this method for the nuclear resonance of $^{57}Fe$ in icosahedral $i$-$Al_{62}Cu_{25.5}Fe_{12.5}$. Our aim was to determine the element-partial VDOS by a purely inelastic method in order to gain more insight into the lattice dynamics of quasicrystals in general and $i$-AlCuFe in particular. We found the surprising result that the Fe-partial $g(E)$ in this system is quite sharply peaked at a certain energy, which was above the broad double maximum which had been found earlier in the neutron-weighted GVDOS found from incoherent inelastic neutron scattering (INS).[14] This result has led us to reconsider the incoherent INS results under a different light, which is the subject of this paper.

The experiments were performed at the cold neutron time-focussing time-of-flight spectrometer IN6 of ILL. At the neutron wavelength of 4.1 Å, this instrument has an elastic energy resolution of 170 $\mu$eV. The maximum momentum transfer is 2.6 Å$^{-1}$, and maximum energy gain of 200 meV (only up scattering is important). The instrument is described in Ref. 46, and on the ILL web site.[47] The experiments at IN6 provide information on the double differential cross section $d^2\sigma/d\omega d\Omega$ which is defined as[46,48]

$$\frac{d^2\sigma}{d\omega\, d\Omega} = \frac{N}{4\pi}\frac{k_f}{k_i}[\sigma_{coh}S(\vec{Q},\omega)+\sigma_{inc}S_{inc}(\vec{Q},\omega)]. \quad (2)$$

Here, $k_i$ and $k_f$ are the initial and final neutron wave vectors, $\vec{Q}=\vec{k}_f-\vec{k}_i$ is the momentum transfer, $\sigma_{coh/inc}$ is the coherent/incoherent neutron cross section, and $S(\vec{Q},\omega)$ and $S_{inc}(\vec{Q},\omega)$ are the coherent and incoherent scattering functions, respectively.[46,48] In the incoherent approximation,[49] we consider only the inelastic incoherent scattering function $S_{inc}^{inel}$. In the case of a monoatomic cubic crystal, this leads to the following relationship for the double differential cross section (see Ref. 48, Chap. 4.4.) for one-phonon inelastic up scattering (phonon annihilation):

$$\frac{d^2\sigma}{d\omega\, d\Omega}\bigg|_{inc,+1}^{inel} = \frac{N\sigma_{inc}}{8\pi M}\frac{k_f}{k_i}Q^2 e^{-2W}\frac{g(\omega)}{\omega}[n(\omega)+1]. \quad (3)$$

$g(\omega)$ is the vibrational density of states for a vibrating mass of $M$ and Debye-Waller factor $W$. $Q$ is the modulus of the scattering vector, and $\omega$ is the energy transfer. When averaged over different atomic species with index $i$, this expression yields the nuclear-partial density of states $g_i(\omega)$ for the $i$th nucleus with scattering cross section $\sigma_i$, Debye-Waller factor $W_i$, and atomic mass $M_i$. In the incoherent approxi-

mation, an average over the reciprocal space is assumed so that the coherent contributions (involving relative motions between two atoms) are lost. This approximation has been found adequate to analyze the data as long as enough data are collected at large $Q$ as compared to the Brillouin zone (for example, see Ref. 50). However, kinematical conditions prevent one from measuring in the region of reciprocal space where the phonon velocity is larger than the neutron velocity: see Figs. 3 and 4 of the first reference in Ref. 14. (For a discussion of the approximations used, see Ref. 51 as well as Ref. 52.) In a quasicrystal, we need to define the pseudo-Brillouin zone (PBZ) constructed from the strongest Bragg diffraction peaks. If each $g_i(\omega)$ is known, then $S_{inc}$ can be calculated, but in fact we need to solve the inverse problem of extracting at least a neutron-weighted $g(\omega)$ knowing $S_{inc}$.

There is a general problem of extracting the single-phonon contribution from the experimentally measured data. The formalism for extracting the multiphonon contributions is similar in both the nuclear scattering (INS) case and the nuclear resonant (INA) case. In the harmonic approximation, knowledge of the effective vibrating mass over different regions of energy is sufficient to estimate the multiphonon contribution. For INA experiments, the question of the effective vibrating mass is quite simple. This makes the multiphonon corrections straightforward. For INS, this is certainly not so: we need some input. In our case, we will show that this can be obtained synergistically from combining (i) the results of our INA iron-partial experiments,[18] and (ii) from comparing INS results for samples with different isotopic substitutions. This allows us to obtain the single-phonon neutron-weighted vibrational density of states $g(E)$. This differs from the corrections made in Ref. 14, where presumably an average atomic mass was used over the whole energy range.

## II. EXPERIMENTAL RESULTS

Our aim in this experiment was to further investigate the discrepancy between the previous inelastic neutron studies of the VDOS in $i$-AlCuFe (Ref. 14) and our iron-partial vibrational density of states experiment.[18] It is known that the composition $i$-$Al_{62}Cu_{25.5}Fe_{12.5}$ produces a stable icosahedral ($i$-) structure over the widest range of temperature, up to at least 1100 K (see Refs. 40 and 42). This makes this composition predestined for a comparative study of phonon (and phason) dynamics. We have studied icosahedral $i$-$Al_{62}Cu_{25.5}Fe_{12.5}$ with various isotopic substitutions. The samples used in this study have already been described in Ref. 53 (other than the isotopic substitutions $^{65}Cu$ and $^{57}Fe$). After melt spinning, they were heat treated to remove the residual $\beta$ phase present in the as-made material, as well as all phason disorder. The quality of all samples was controlled using x-ray diffraction. Peak positions, intensities, and linewidths were found characteristic of high-grade multidomain icosahedral samples (flakes). At the Nuclear Resonance Beamline ID18 (see Ref. 54) of the ESRF, we previously studied the nuclear-resonant inelastic absorption (INA) of synchrotron radiation by the $^{57}Fe$ nuclei in an $^{57}Fe$ enriched sample (natural Cu).[18] At the time-of-flight inelastic beamline IN6 of ILL,[47] we studied the neutron-weighted GVDOS, presented here. The samples were contained in standard thin-walled aluminum cans. INS spectra were taken

TABLE I. Effective composition-weighted nuclear cross sections for samples in barns. The total cross section is defined as $\sigma_{tot} = \sigma_s + \sigma_a$ where $\sigma_s$ is the total (coherent plus incoherent) scattering cross section and $\sigma_a$ the absorption cross section at a neutron wavelength $\lambda = 4.12$ Å (Ref. 55). Samples of the INS experiment are labeled a, b, and c.

| Sample | Cu | Fe | $\sigma_s^{Al}$ | $\sigma_s^{Cu}$ | $\sigma_s^{Fe}$ | $\sigma_a$ | $\sigma_{tot}$ |
|---|---|---|---|---|---|---|---|
| a | nat | nat | 0.931 | 2.05 | 1.45 | 3.266 | 7.698 |
| b | 65 | nat | 0.931 | 3.70 | 1.45 | 2.325 | 8.408 |
| c | nat | 57 | 0.931 | 2.05 | 0.13 | 3.243 | 6.348 |

on three samples with different isotopic enrichment in order to change the contrast mainly between Cu and Fe: sample a, natural Cu and Fe; b, $^{65}$Cu, natural Fe; c, natural Cu, $^{57}$Fe. Sample a was considered the reference. The composition-weighted neutron-scattering cross sections are given in Table I (see Ref. 55). That of sample b was strongly increased: high sensitivity to Cu. The cross section of sample c was decreased: insensitivity to Fe. Measurements using a neutron wavelength of 4.12 Å at 300 and 600 K were compared to detect any significant anharmonic effects. The empty sample can was also measured at 300 and 600 K and this signal removed. The counted neutrons were summed over the full range of angles accessible at IN6. The edge of the elastic peak was removed using the measured vanadium standard signal.

Figure 1 gives the experimental generalized frequency distributions for samples a, b, and c at 300 (left) and at 600 K (right) with the empty can data already subtracted and the edge of the elastic peak removed. These curves have been normalized by the sample mass, the time and neutron flux, as well as detector efficiency. We observe the dramatic increase in the height of the first peak with increasing copper cross section (sample a to b), and decrease in the second peak with decreasing iron cross section (sample a to c). Due to the fact that these peak structures are broad, there is also an overall

effect as well. However, we can conclude that the most important cross section for the energy region of the first peak is that of copper, and for the second that of iron. This is our starting point to calculate the multiphonon contributions. Using a formalism similar to the case of INA,[56] the multiphonon signal was calculated assuming bands in energy of different effective atomic masses. It was found necessary and sufficient to assume a low-energy band of atomic mass given by Al and Cu (atomic mass a.m. 44, position $\langle E \rangle$ ~14 meV), a middle band given by Al and Fe (a.m. 35, $\langle E \rangle$~28 meV) , and an upper band of only Al (a.m. 27, $\langle E \rangle$~41 meV). It is clear that this is consistent with the raw data. In addition, it is consistent with the previous iron-partial $g(E)$ results as well, which were highly peaked at the upper peak of the neutron raw data. Figure 2 gives the experimental generalized frequency distribution for sample a at 300 and at 600 K. The multiphonon as well as the background intensities calculated in this way are also shown. This last contribution is essentially a constant level in the time-of-flight spectra, a reasonable assumption since one cannot completely remove the frame-overlap signal.[46] By subtracting these two latter contributions from the uncorrected GV-DOS, we arrive at the neutron-weighted vibrational density of states $g(E)$. This is then normalized to have unit area.

Figure 3 shows (a) the 300-K and (b) the 600-K neutron-
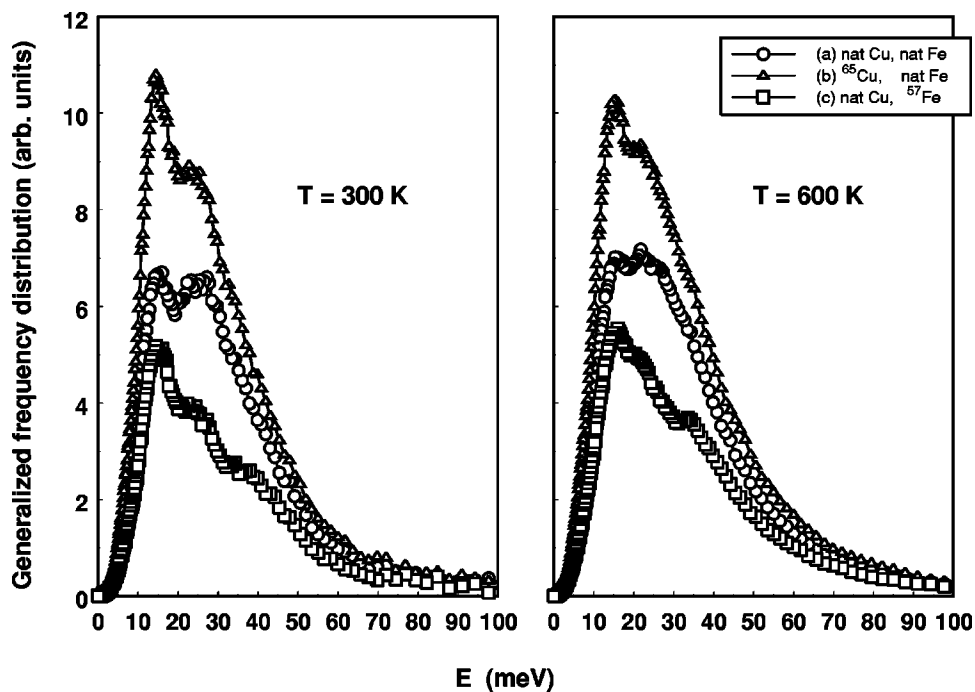


FIG. 1. The experimental generalized frequency distributions of samples a, b, and c at (left) 300 K and (right) 600 K.
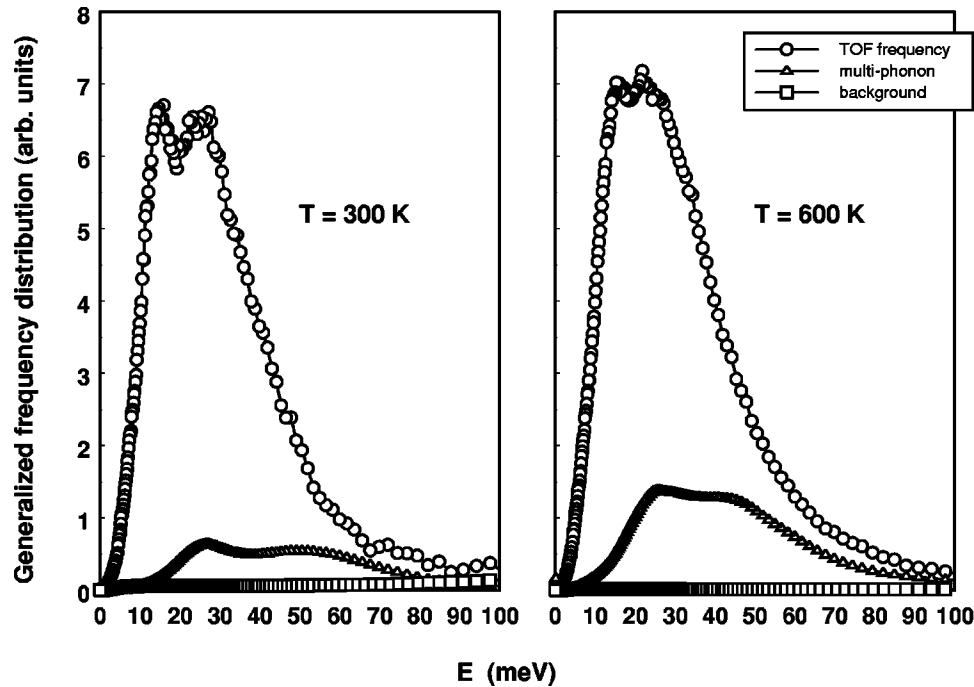
FIG. 2. The experimental generalized frequency distributions of sample a at (left) 300 K and (right) 600 K. Shown as well are the calculated multiphonon and background intensities which have to be subtracted to arrive at the vibrational density of states $g(E)$.

weighted $g(E)$ curves as corrected for multiphonon effects as well as the Debye-Waller factor. Henceforth we will reserve the term GVDOS for the uncorrected neutron data. The curve for the sample a can be directly compared to the previous GVDOS results of Klein *et al.*,[14] which were, however, corrected for multiphonon effects by assuming a constant atomic mass over energy. The multiphonon corrections presented above have reduced the previously observed *upper maximum* near 22 meV into the *broad plateau* shown here. Thus this maximum is mostly due to multiphonon contributions. Comparing the three samples, the strongest effect on $g(E)$ of the different scattering cross sections is the *increase* in the relative intensity of the first peak at about 14–15 meV

and a systematic *loss* in intensity near the high-energy plateau for increasing Cu and decreasing Fe scattering cross section. This is the same conclusion which we made from considering the raw data presented in Fig. 1. However, now this second maximum is practically absent in the neutron-weighted $g(E)$, which is heavily weighted by copper and aluminum. The second point is that the results for $g(E)$ in all three samples at a given temperature superpose in the region from zero up to about 8 meV. There is thus little dependence on the relative scattering cross section in this region.

Figure 4 shows a comparison of the neutron-weighted $g(E)$ measured on sample c and the previously published iron-partial $g(E)$ (see Ref. 18: both have multiphonon com-
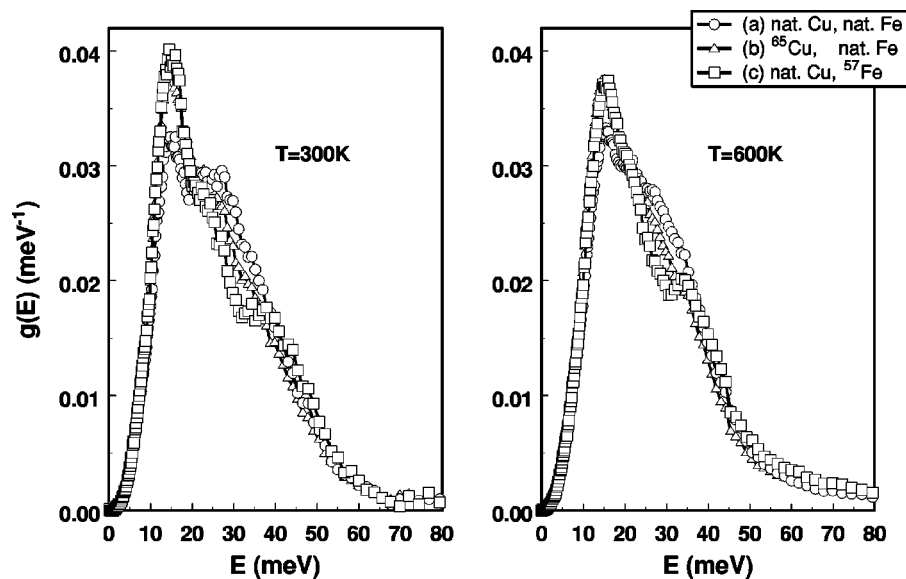


FIG. 3. The neutron-weighted $g(E)$ (INS) for the three samples a, b, and c at 300 K (left) and 600 K (right). Corrections have been made for the multiphonon and background contributions.
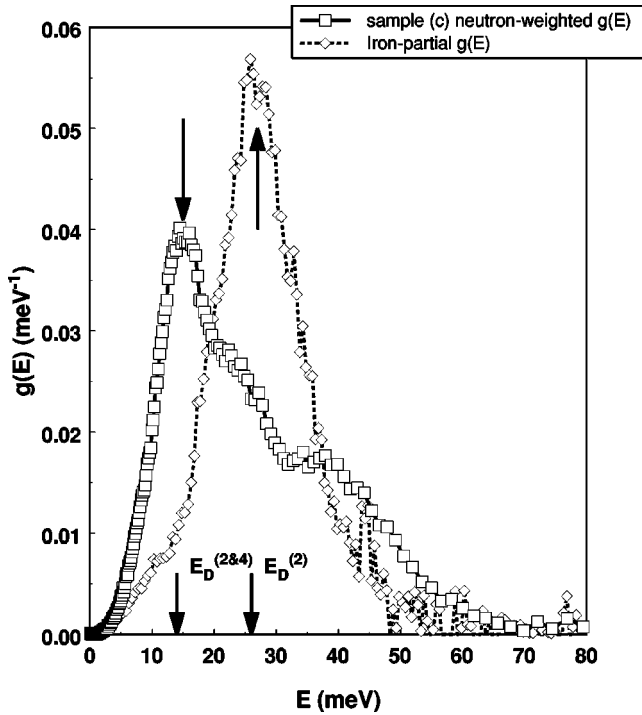
FIG. 4. The neutron-weighted $g(E)$ (INS) of sample c as compared to the iron-partial $g(E)$ (INA). Top of figure: the lower peak of the neutron-weighted $g(E)$ curve is marked with an arrow at 15 meV, and the peak of the iron-partial $g(E)$ result at 27 meV. Bottom of figure: the two arrows mark the Debye cutoff energy $E_D$ as calculated with the quadratic term (2) only, or the quadratic and quartic terms (2&4) in $g(E)$ at low $E$, as discussed in the text.

ponents deleted). The most striking feature of this figure is the difference in positions of the rather sharp maxima: at about 14–15 meV for the neutron-weighted $g(E)$ data and at about 27 meV for the iron-partial $g(E)$, both marked with arrows in the figure. (Both curves have been normalized to unit area.) The maximum of the iron-partial $g(E)$ lies at the upper edge of the plateau found in the neutron-weighted $g(E)$ curve of sample a, while this plateau progressively decreases going from sample a to b to c. The second striking feature in this comparison is the low intensity of the iron-partial VDOS in the *low-energy* region up to (and actually above) the maximum observed in the neutron-weighted $g(E)$ as compared to the intensity at larger energies.

## III. DISCUSSION

From a comparison between our data on the iron-partial $g(E)$ and the GVDOS of Klein *et al.*,[14] we previously made[18] the simple conclusion that the upper maximum is dominated by Fe, and the lower one by Cu. We have now presented different data for isotope-substituted samples with the same composition. A comparison of the raw data from these samples strongly reinforces this simple conclusion. Sample b is characterized by a stronger weighting for Cu and sample c a smaller weighting for Fe. In both cases, the GV-DOS (Fig. 1) sharpens considerably in the region of the maximum near 14–15 meV. Since, as is clear from the composition (and the structure model discussed in the Introduction), the nearest neighbors of both Cu and Fe must be domi-

nated by Al, we can conclude that the energy range of the lower peak is dominated by Al and Cu while that of the upper by Al and Fe. In addition, the multiphonon calculations show the presence of a broad region at even higher energies dominated by Al. We observe as well that the neutron-weighted $g(E)$ tends to be as sharply peaked, but at lower energy, as that observed for the iron-partial $g(E)$. The simplest physical interpretation of this difference between iron and copper would be based on a different stiffness coefficient: that for Fe with its neighbors being larger than that for Cu with its neighbors. This difference would then be related to the different local environments for Fe and Cu in the Katz-Gratias model of $i$-AlCuFe,[39] described above. It is known that above about 10 meV, the phonon dispersion curves for quasicrystals are composed of an overlap of acoustic and optical, and, perhaps, critical modes. This makes an interpretation in terms of acoustic phonons difficult. Thus we will in the following first make model-free conclusions on the thermal properties and average stiffness coefficients. But to understand the differences between the (Al and Cu dominated) neutron-weighted $g(E)$, and the iron-partial $g(E)$, we must consider the differences in local structure between Cu and Fe as well.

### A. Comparing the Debye temperatures

The vibrational density of states is expected to be Debye-like in the low-energy limit. From this, we can extract the Debye temperature $\Theta_D$ from the quadratic term in $g(E)$. We define the Debye-model density of states extending up to a Debye cutoff $E_D$ as:

$$g_D(E) = \begin{cases} a^{(2)}E^2, & E \in \{0, E_D\} \\ 0 & \text{otherwise} \end{cases}, \qquad (4)$$

where the constant $a^{(2)}$ is given by the normalization of $g(E)$ as $3/E_D^3$ and the Debye temperature $\Theta_D$ as $k_B\Theta_D = E_D$. Thus we take the zero energy limit as

$$\lim_{E \to 0} \frac{g(E)}{E^2} = a^{(2)} = \frac{3}{E_D^3} \qquad (5)$$

which gives the Debye temperature $\Theta_D$ in terms of the low-energy limit of $g(E)$. In such a model, the experimental $g(E)$ is replaced by the Debye expression, Eq. (4). The next higher approximation would be to add a quartic term: $g(E) = a^{(2)}E^2 + a^{(4)}E^4$. In this case, we must change the expression for the Debye energy calculated from the normalization of $g(E)$: $a^{(2)}E_D^3/3 + a^{(4)}E_D^5/5 = 1$. In order to extract such a quartic term, in Fig. 5 we plot $g(E)/E^2$ for the three neutron-weighted $g(E)$, as well as the iron-partial $g(E)$ as a function of $E^2$. The low-$E^2$ region is fitted with a linear function in $E^2$ yielding $a^{(2)}$ and $a^{(4)}$. All results give nearly the same intercept, yielding nearly the same $a^{(2)}$, and thus in the simplest model, the same Debye temperature and denoted $\Theta_D^{(2)}$. These are all presented in Table II. However, the values obtained for the extended model including the quartic term for the neutron-weighted $g(E)$ are much smaller. These are denoted $\Theta_D^{(2\&4)}$. Since the quartic term is virtually absent from the iron-partial $g(E)$, here there is no change. Also shown in
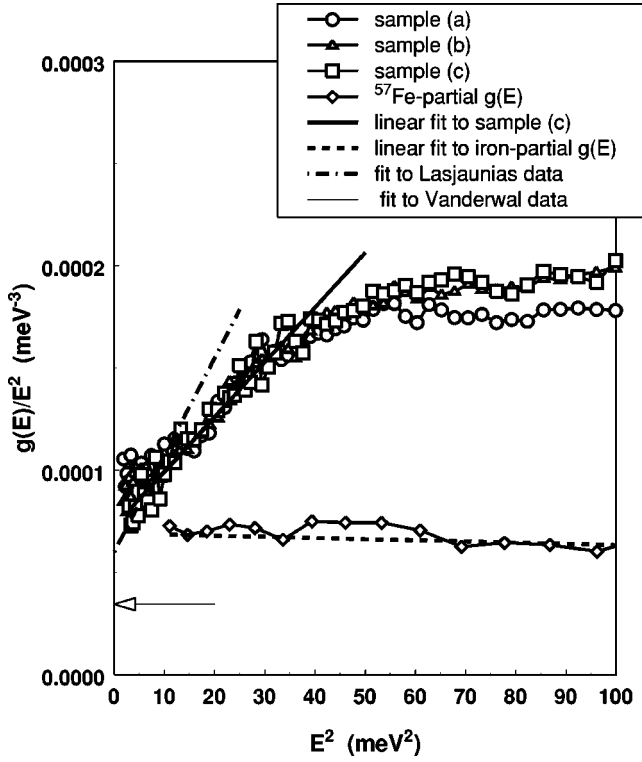
FIG. 5. The low-energy region of the neutron-weighted $g(E)$ (INS) as compared to iron-partial $g(E)$ (INA). Plotted is $g(E)/E^2$ as a function of $E^2$. Linear fits to both are also shown. Also shown are the predictions from the measured low-temperature lattice specific heat (Lasjaunias *et al.* Ref. 21), and (arrow) room-temperature sound velocity from Brillouin scattering (Vanderwall *et al.* Ref. 57). The former are calculated from the parabolic fit shown in Fig. 7.

the table are the Debye temperatures as calculated from the average over the whole $g(E)$ in the usual way:

$$\langle E \rangle \equiv \int_0^\infty E g(E) dE = \frac{3}{4} k_B \Theta_D^{(\langle E \rangle)} . \qquad (6)$$

These results are similar to those calculated from Eq. (5) except that for the iron-partial $g(E)$ which is much higher. The rest of the figure and remaining data in the table will be discussed below.

Another expression for the Debye temperature in the zero-energy, zero-wave-vector limit is provided by the (Debye) average sound velocity $v_D$. This is the average over the longitudinal and transverse sound velocities $v_l$ and $v_t$, respectively. For icosahedral symmetry these are isotropic so that

this average is given by $3/v_D^3 = 1/v_l^3 + 2/v_t^3$. Unfortunately, we have not been able to find such results for exactly our composition $i$-$Al_{62}Cu_{25.5}Fe_{12.5}$, and as we shall discuss later, such results are sensitive to composition as well as temperature. Quilichini and co-workers[5,12,13] give results on the phonon dispersion curves for the composition $i$-$Al_{63}Cu_{25}Fe_{12}$ measured by coherent neutron scattering. They report[5] $v_t = 3650$ m/s and $v_l = 7700$. From this we obtain $v_D = 4106$ m/s. However, due to the small sample used, their data are not too accurate and even different velocities $v_l$ and $v_t$ have been extracted from these same dispersion curves.[21] Vanderwal *et al.*[57] report on room-temperature Brillouin scattering from $i$-$Al_{63.5}Cu_{24.5}Fe_{12}$. This method is highly surface sensitive but the authors present arguments for their interpretation of bulk values of the velocity. They report $v_t = 3809$ m/s and $v_l = 7191$. From this we obtain $v_D = 4257$ m/s. The usual expression for $\omega_D$ is

$$k_B \Theta_D = v_D \left( 6\pi^2 \frac{N}{V} \right)^{1/3} .$$

These results yield a Debye temperature of 495 K for the results of Quilichini *et al.* and 514 K from those of Vanderwal *et al.* These are shown compared to other determinations in Table III. Thus for $i$-AlCuFe *there is a discrepancy in the Debye temperature as calculated from the VDOS $g(E)$ and from the sound velocity $v_D$*. It must be emphasized that the iron-partial $g(E)$ and the neutron-weighted $g(E)$ data presented here have been corrected for multiphonon effects and in all cases we have been very careful not to distort the data in the low-energy region. In the usual case, these two different determinations of the Debye temperature do agree well within experimental errors. The discrepancy found here is in the same direction as that found in Ref. 22: we find a larger Debye temperature or smaller $C_{latt}$ term calculated from the sound velocity. Additionally in Table III we give the Debye temperature as calculated from standard Mössbauer spectra using the Lamb-Mössbauer factor (LMF) and the second-order Doppler shift (SOD).[43] Since these involve other powers of $E$ in the integration over $g(E)$, there is little agreement with our data presented in Table II.

We shall compare the calculations of the Debye temperature as determined from the lattice specific heat $C_{latt}$ below. It has been found that $C_{latt}$ depends sensitively on the state of the sample.[20,21] Thus we want to consider results for $i$-AlCuFe at the same composition and in the highly annealed state. The x-ray-diffraction spectra show no additional phases, and the line positions, widths, and intensities are characteristic of phason-free icosahedral phases.[42] The re-

TABLE II. $a^{(n)}$: Coefficients of the linear fit to $g(E)/E^2$ as a function of $E^2$. $\Theta_D$: Different values of the Debye temperature. Source: (2): from low-$E$ quadratic term; (2&4): including both square and quartic terms; ($\langle E \rangle$): from average of $E$ over the $g(E)$ (INA $^{57}$Fe); INS, samples a, b, c.

| Sample | $a^{(2)}$ $10^{-4}$ meV$^{-3}$ | $a^{(4)}$ $10^{-6}$ meV$^{-5}$ | $\Theta_D^{(2)}$ K | $\Theta_D^{(2\&4)}$ K | $\Theta_D^{(\langle E \rangle)}$ K |
|---|---|---|---|---|---|
| $^{57}$Fe | 1.43 | −0.37 | 319 | 319 | 430 |
| a | 1.77 | 5.50 | 298 | 173 | 309 |
| b | 1.69 | 5.81 | 302 | 171 | 297 |
| c | 1.78 | 5.50 | 297 | 173 | 297 |

TABLE III. Different values of the Debye temperature $\Theta_D(K)$. $\beta$: from the $T^3$ term in the fit to the lattice specific heat; $\beta \& \delta$: from the fit to the lattice specific heat using both the $T^3$ and $T^5$ terms; $v_s$: from sound velocity as from either neutron scattering ($n$) or Brillouin scattering ($B$) results; LME: from Lamb-Mössbauer factor; SOD: from second-order Doppler shift (the latter two from conventional Mössbauer spectroscopy). Power: power of $E$ involved in the average over the density of states $g(E)$.

| Source | $\beta$ | $\beta \& \delta$ | $v_D^n$ | $v_D^B$ | LME | SOD |
|---|---|---|---|---|---|---|
| Reference | 21 | 21 | 5 | 57 | 43 | 43 |
| Power | | | 1 | 1 | $-1$ | 1 |
| $\Theta_D$ (K) | 427 | 185 | 495 | 514 | 550 (10) | 580 (10) |

sults of Lasjaunias et al.[21] have shown that $C_{latt}$ is also very sensitive to composition. However, they also present results for the same composition as studied here. Possible magnetic contributions (which would affect the specific heat much more than the INS, or INA, experiments) were checked for with sensitive susceptibility studies in a superconducting quantam interference device magnetometer and found not to be present.

## B. Lattice dynamics and thermal properties

We will now compare our results for the vibrational density of states $g(E)$, and thermal properties. The vibrational part of the internal energy per atom can be expressed in terms of $g(E)$ as[58,59]

$$U = \frac{3}{2} \int_0^\infty E g(E) \left( \frac{e^{\beta E} + 1}{e^{\beta E} - 1} \right) dE. \tag{7}$$

In the above, $\beta = 1/k_B T$, where $k_B$ is the Boltzmann constant and $T$ the temperature, and this expression includes the zero-point motion through the Bose factor in parentheses. If we neglect the temperature dependence of the density of states (which we do in the following), then the temperature differential of $U(T)$ yields the constant-volume lattice specific heat per atom:

$$C_V = 3k_B \int_0^\infty g(E) \left( \frac{\beta E}{e^{\beta E} - 1} \right)^2 e^{\beta E} dE. \tag{8}$$

The vibrational entropy per atom can be calculated from

$$S = -3k_B \int_0^\infty g(E) \left[ \frac{\beta E}{2} \left( \frac{e^{\beta E} + 1}{e^{\beta E} - 1} \right) - \ln(e^{\beta E/2} - e^{-\beta E/2}) \right] dE. \tag{9}$$

The mean square atomic displacements can be calculated from

$$\langle (\Delta x)^2 \rangle = \frac{\hbar^2}{2M} \int_0^\infty \frac{g(E)}{E} \left( \frac{e^{\beta E} + 1}{e^{\beta E} - 1} \right) dE. \tag{10}$$

Notice that this expression contains the atomic mass $M$, so that for each atomic species we should use the element-partial $g(E)$ as well. This is only completely known for iron, but the neutron-weighted $g(E)$ should give a very good approximation for copper. The (temperature-independent) mean force constant $V$ can be calculated from

$$V = \frac{M}{\hbar^2} \int_0^\infty g(E) E^2 \, dE. \tag{11}$$

(If the above integrals are calculated in energy units of meV, then a useful constant is $\hbar^2/M \simeq 0.052$ meV nm$^2$/A, where $A$ is the atomic mass.) Again, this does depend on $M$, so that the element-partial $g(E)$ should be substituted. However, we expect that the neutron-partial $g(E)$ gives a good estimation of the average value for copper. The resulting vibrational contributions to the internal energy $U$, specific heat $C_{latt}$, entropy $S$, mean square displacement $\langle (\Delta x)^2 \rangle$, and average force constant $V$ are given in Table IV. Representative values are give for 0 and 300 K. We make the following observations of these results. At 300 K, the kinetic contribution to $U$

TABLE IV. Results for averages over the $^{57}$Fe-partial and neutron-weighted $g(E)$ results of the samples a, b, and c. The average force constant $V$ is independent of temperature. A is the relative atomic mass. $U$ is the vibrational-contribution to the internal energy. $C_{latt}$ is the lattice specific heat. $S$ is the vibrational contribution to the entropy. $\langle (\Delta x)^2 \rangle$ is the mean-square displacement.

| Sample | $T$ K | $V$ A meV/nm$^2$ | $U$ meV/atom | $C_{latt}$ $k_B$/atom | $S$ $k_B$/atom | $\langle (\Delta x)^2 \rangle$ nm$^2$/A |
|---|---|---|---|---|---|---|
| $^{57}$Fe | 0 | 541 | 42.23 | | | 0.00107 |
| | 300 | | 85.80 | 2.70 | $-3.08$ | 0.00320 |
| (a) | 0 | 526 | 41.04 | | | 0.00126 |
| | 300 | | 86.10 | 2.70 | $-3.37$ | 0.00635 |
| (b) | 0 | 506 | 39.46 | | | 0.00135 |
| | 300 | | 85.61 | 2.71 | $-3.49$ | 0.0188 |
| (c) | 0 | 516 | 40.23 | | | 0.00131 |
| | 300 | | 85.95 | 2.70 | $-3.46$ | 0.00718 |
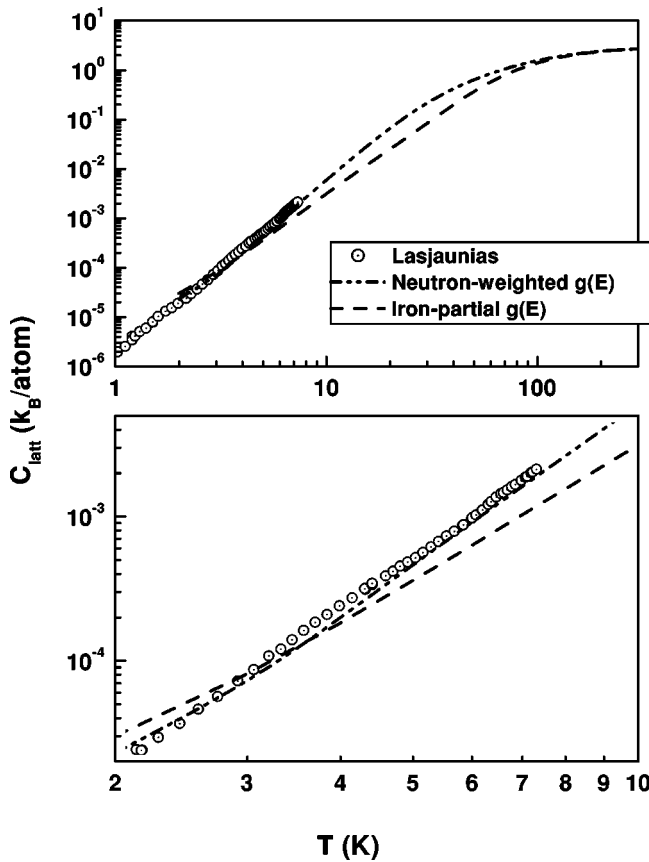
FIG. 6. Lattice specific heat calculated from the neutron-weighted and iron-partial $g(E)$ results as compared with the experimental results of Lasjaunias *et al.* Ref. 21, in a log-log plot. The upper curve shows the correct high-temperature limit ($3k_{\mathrm{B}}$/atom). The lower curve shows the comparison in more detail.



FIG. 7. Lattice specific heat calculated from the neutron-weighted and iron-partial $g(E)$ results as compared with the experimental results of Lasjaunias *et al.*, Ref. 21 as $C_{\mathrm{latt}}/T$ vs $T^2$. A parabolic fit though the experimental data is also shown. This is used to calculate the expected $g(E)$ at low $E$ as shown in Fig. 5.

and $C_{\mathrm{latt}}$ are essentially equal for all four results. There is a difference in the entropy, with that calculated from the iron-partial $g(E)$ being the smallest. We will see this reflects differences in the low-temperature lattice specific heat per atom as calculated from the different $g(E)$. Also we note the large differences between the mean square atomic displacements, especially with increasing temperature. The results from the neutron-weighted $g(E)$, especially sample (b), are over twice that found from the iron-partial $g(E)$. Notice that sample b has the largest copper cross section, so that in this result both the iron and aluminum contributions are decreased compared to sample a. The average force constant for the iron-partial $g(E)$ is also significantly larger than those for the neutron-weighted results. Note the correlation between these two latter results $\langle(\Delta x)^2\rangle$ and $V$, despite the fact of the energy weighting factors being quite different [see Eqs. (10) and (11)].

We show in Fig. 6 the lattice specific heat at constant volume $C_{\mathrm{latt}}$ at low temperature as calculated from the neutron-weighted $g(E)$ of sample c, as well as from the iron-partial $g(E)$ in a log-log plot. The results calculated for the three different neutron-weighted $g(E)$ results do not differ in the temperature range shown due to the fact that they are dominated by the low-energy limit of $g(E)$. [The calculated results below 2 K are not reliable due to the extreme weighting of the very low energy range of $g(E)$.] The $C_{\mathrm{latt}}$ result

from the iron-partial $g(E)$ follows a $T^3$ behavior in this range, while that for the neutron-weighted $g(E)$ (dominated by Al and Cu) shows a larger slope. These calculations are also compared to the experimental results of Lasjaunias *et al.*[21] for icosahedral *i*-AlCuFe with the same composition. The $C_{\mathrm{latt}}$ per atom as calculated from the neutron-weighted $g(E)$ is *practically identical* both in slope and magnitude with the experimental result in this range, while that calculated from the iron-partial $g(E)$ lies somewhat below. This is a quite surprising result in that the noninteger power of $T$ proposed by Lasjaunias *et al.*[21] has been very difficult to understand. The lattice specific heat presented by Lasjaunias *et al.* deviates from the Debye result (cubic term) at anomalously low temperatures. This is the reason why the authors did not try to estimate a Debye temperature from their data.[60] The very low-temperature region was analyzed in terms of a nuclear quadrupole contribution $C_{\mathrm{n}}T^{-2}$ and an ``electronic'' contribution of $AT^{0.88}$. This sublinear deviation from the usual linear electronic contribution may be the result of two level systems (see Ref. 61 for a discussion of this in the case of *i*-AlPdRe), but does make the analysis difficult. It is also known that polycrystalline *i*-AlCuFe quasicrystals (such as used for the specific-heat measurements) often contain small amounts of paramagnetic impurities as well which would strongly disturb such sensitive specific-heat measurements. In addition, the measured specific-heat as presented in Ref. 21 is extremely sensitive to small changes in composition. Since the measured $C_{\mathrm{latt}}$ is compatible with the vibrational specific heat as calculated from our measured neutron-weighted $g(E)$, these problems do not seem to adversely affect the results presented in Ref. 21.

In order to further test this equality in experimental and calculated lattice specific heat, we show in Fig. 7 the usual plot of $C_{\mathrm{latt}}/T$ as a function of $T^2$ (note we use the units of the Boltzmann constant $k_{\mathrm{B}}$ proatom). This emphasizes the differences at higher temperatures as compared to Fig. 6. Shown as well are the results from the neutron-weighted and the iron-partial $g(E)$ calculations. Again, the neutron-weighted results are quite close to the experimental ones. Lasjaunias *et al.* found that the usual model for the specific

heat, given by Eq. (1), did not work in general for the different compositions of $i$-AlCuFe studied, and instead found for the same composition as studied here (not including the nuclear term)

$$C_p = AT^{0.88} + BT^{3.55}. \tag{12}$$

Thus the physical interpretation of the two contributions is not very straight-forward. The first contribution may not only be due to the conduction electrons but to that of TLS known from insulating glasses, which we briefly discussed above. The second contribution, with the exponent of 3.55, cannot simply be due to extended acoustical phonon states. This conclusion is further supported by a similar noninteger power-law $BT^{3.87}$ for the "lattice" contribution in the nearby composition $i$-$Al_{63}Cu_{25}Fe_{12}$, obeyed in an even larger temperature interval (between 0.7 and $\sim 12$ K). In this case, the interpretation of the specific-heat data is more straight-forward because of a strictly linear variation of the "electronic" contribution below 1 K. In addition, the comparison to the acoustic limit as estimated from the sound velocity is more correct, as data are available for this composition.[57] For both compositions, Lasjaunias $et\ al.$ concluded that in the low-temperature range ($T < 3$ K), a strictly Debye-like cubic term does not work.[60] However, in order make a comparison with results of the neutron-weighted and iron-partial $g(E)$, we shall fit the "lattice" contribution proportional to $BT^{3.55}$ by the sum of the usual $T^3$ and $T^5$ terms as in Eq. (1). From this we can calculate an effective $g(E)/E^2$. The polynomial fit to the experimental data is shown in the figure: $C_{latt}/T = \beta T^2 + \delta T^4$. This results in $\beta = 2.99\,093 \times 10^{-6} k_B/$atom K$^3$, and $\delta = 4.7196 \times 10^{-8} k_B/$atom K$^5$. The usual expression for $\beta$ in terms of the Debye temperature is $\beta = (12\pi^4/5) N_A k_B / \Theta_D$. This yields a Debye temperature of 427 K, significantly above that found from the quadratic dependence of $g(E)$ at low $E$ (Table II). By substituting the extended Debye model including square and quartic terms into the expression for the specific heat, in Eq. (8) we arrive at expressions for $\beta$ and $\delta$ in Eq. (1):

$$\beta = \frac{4}{5}(\pi k_B)^4 a^{(2)}, \tag{13}$$

$$\delta = \frac{16}{7}(\pi k_B)^6 a^{(4)}. \tag{14}$$

These can be used to calculate a "Debye" temperature using both $\beta$ and $\delta$, given in Table III, much smaller than the above. In addition, we can now calculate an equivalent $g(E)/E^2$. This is given by the dash-dot line in Fig. 7. Although the agreement with the experimental $g(E)$ is not very good, it must be remembered the numerous approximations involved [sublinear "electronic" term, leading two terms only in $g(E)$ and specific heat, as well as the remaining neutron cross section weighting in $g(E)$, etc.]. The arrow is the result for the zero energy limit from the sound velocity reported by Vanderwal $et\ al.$ from Brillouin scattering[57] at room temperature. This is significantly below the intercept of the measured $g(E)$, and that predicted from the specific heat. These differences from the zero energy limit of the $measured$ $g(E)/E^2$ are a strong indication of nonacoustic excitations down to arbitrarily small energies. Note that the sound ve-

locity used was measured at room temperature.[57] However, the sound velocity, and thus also the calculated $\Theta_D$, increase at lower temperature (see Refs. 26, 27, and 62), so that the predicted $g(E)/E^2$ would decrease. The effect is about 6% between room temperature and 4 K. This would, however, only increase the differences with the measured $g(E)$ discussed here.

We have seen that in the low-energy region, the neutron-weighted $g(E)$ can be expressed as a sum of a square and quartic terms. The power of $T^{3.55}$ for $C_{latt}$ proposed by Lasjaunias $et\ al.$[21] might be seen as well as a superposition of the resulting $\beta T^3$ and $\delta T^5$ terms in $C_{latt}$ which could not be resolved because of the fact that the quartic term in $g(E)$ is unusually large. However, a simple interpretation of the neutron-weighted $g(E)$, with square and quartic terms, is complicated by the fact that the iron-partial $g(E)$ does not show any anomalous quartic term in the low-energy region (below ca. 10 meV). Thus iron does not participate in these extra excitations. Previously,[22] this quartic term in $g(E)$ had been calculated from specific-heat results in $i$-AlPdMn quasicrystals in the temperature range of 1.6–14 K. It was interpreted in terms of the leading deviation from linearity in the transverse acoustic (TA) phonon dispersion relation. The quartic term $b$ is given by $-5\alpha_t/(\pi^2 v_t^6)$ in the above.[22] The constant $\alpha_t$ is related to the first deviation from linearity in the dispersion relation $E/\hbar = \omega(k) = v_t k + \alpha_t k^3$. The results for the iron-partial $g(E)$ are, however, in contradiction to this explanation. It is not reasonable to conclude that the $extended\ acoustic\ phonons$ are so different at copper than at iron sites in the energy range up to 10 meV. Thus this result suggests that there is a significant $nonacoustic$ contribution to the vibrational density of states at arbitrarily low energies. From the results on theoretical models,[5] critical modes, that is, almost spatially confined lattice excitations, are expected at high energy. These modes would then be at least partially localized in reciprocal space as well, and would not follow any dispersion curve. They result from the essentially infinite number of van Hove singularities.[5] In these calculations, such singularities exist as well down to low energy, but with such diminishing weight that they are not expected to disturb the Debye limit of the acoustic phonons. From our results, we propose that $even\ in\ the\ low-energy\ limit$, there must be many such critical modes in icosahedral $i$-AlCuFe (and thus in quasicrystals in general). These modes would strongly affect the thermal properties such as the low-temperature specific heat. The direct evidence which we present here is the difference in the quartic term in the vibrational $g(E)$ between the neutron-weighted and the iron-partial $g(E)$. In addition, there is a large difference in the measured zero energy limit of $g(E)/E^2$ as compared to the value calculated from the sound velocity. This term also leads to the unusual low-temperature lattice contribution to the specific heat as measured by Lasjaunias $et\ al.$,[21] which is in good agreement with the predictions of the neutron-weighted $g(E)$. The small residual differences seen in Fig. 7 may be due to approximations involved in subtraction off the electronic contribution to $C_V$, or to the weightings of the neutron scattering cross sections of $g(E)$ still remaining.

The origin of the different properties at iron and copper sites may lie in the different local structures in the model of Katz and Gratias. A significant feature of this model is the

copper present on the $bc$ sites, which turn out to be at the center of an Al icosahedron. It seems that these copper atoms can move rather freely as evidenced by the larger mean square displacements and smaller average force constants (see Table IV) and by the quartic term in the neutron-weighted $g(E)$.

We now want to compare the properties of $g(E)$ at low $E$, and the positions of the sharp maxima. For this, we calculate the Debye cutoff energy $E_D$ as predicted from the $a^{(2)}$ term alone, or including $a^{(4)}$ in the $g(E)$ expansion. These are shown as the lower arrows in Fig. 5. They agree reasonably well with the maximum in the iron-partial and the neutron-weighted $g(E)$, respectively. Thus the presence of the quartic term in $g(E)$, and the significantly lower position of the sharp maximum correlate with each other. The square term in $g(E)$ alone is related to the higher maximum seen for the iron-partial $g(E)$. We are then forced to conclude that the copper are significantly less rigidly bound in the quasilattice than the iron atoms, and this is related to the presence of nonacoustic elementary excitations present at the copper (and aluminum), but not the iron sites. The comparison with the calculations based on the speed of sound $v_D$ indicate that there may be further such nonacoustic excitations on iron sites as well. However, $v_D$ has been determined in a sample with a slightly different composition.

It is interesting to note that it is also the same copper atoms which should be responsible for the very high phason jump rates measured for Cu by quasielastic neutron scattering (QNS).[44] It is also significant that local tunneling states have also been observed in icosahedral AlCuFe as well. Bert et al.[26] have reported evidence of TLS (tunneling states) from measurements of changes of velocity and attenuation of acoustic waves. These local tunneling states could very well be *dynamical* phason tunneling (rather than static phason defects which they ruled out). As reported by Dolinšek et al.,[63] aluminum phason jumps can be observed down to very low temperatures by two-dimensional NMR correlation spectroscopy. In the assisted phason jump model of Coddens,[44] the aluminum jumps allow copper jumps to occur. The recent QNS studies on single-grain $i$-AlPdMn (Ref. 64) have shown that at least some phason jumps are collective events between several nearby atoms. We reached the same conclusions for the high-temperature range for iron using quasielastic Mössbauer spectroscopy.[43] It is feasible that local phason-phonon coupling at copper sites then leads to the excess local fluctuations seen here. If such a model is correct, it would mean that aluminum and/or copper sites are affected over all energy scales by such dynamical tunneling, but not iron sites at least at these temperatures. Recent numerical[65] studies have demonstrated that the phason-phonon coupling parameter to be non-negligible. Thus a phonon-phason mode might provide an alternative scenario to explain our results, in addition to the one considering the almost localized ''critical'' modes.

## IV. CONCLUSIONS

We have presented time-of-flight inelastic neutron-scattering results on the lattice dynamics of the icosahedral quasicrystal $i$-Al$_{62}$Cu$_{25.5}$Fe$_{12.5}$ with various isotopic substitutions. By combining the scaling of the experimental generalized frequency distributions with changes in nuclear cross sections, we were able to model the effective atomic masses over the energy range of the VDOS, allowing us to make more detailed multiphonon corrections than previous studies. By doing this, we were able to show that the neutron-weighted vibrational density of states $g(E)$ is sharply peaked, in contrast to earlier conclusions. However, the neutron-weighted $g(E)$ differs considerably from the iron-partial $g(E)$ which we presented previously.[18] Since the neutron-weighted $g(E)$ is sensitive practically to Al and especially Cu, this shows that the partial vibrational density of states differ greatly between Cu and that of Fe. The results for different thermal properties as calculated from the different neutron-weighted and iron-partial $g(E)$ results lead to several conclusions. All results show the same initial Debye-like quadratic term, yielding the same lattice Debye temperature $\Theta_D$. The calculated lattice specific heat reproduces the measured low-temperature lattice specific heat previously published.[21] We conclude that the quartic term in the neutron-weighted $g(E)$ is due to the presence of nonacoustic vibrational elementary excitations mainly on copper and aluminum. A possible reason for the large differences in lattice-dynamical properties between copper and iron is suggested by differences in lattice site occupations in the perfect icosahedral crystal model of Katz and Gratias.[39,41] One result of these studies is the evident need for numerical studies of the atomic-partial vibrational density of states in icosahedral models. Mihalkovič et al.[66] have recently started such a study of approximant structures for the decagonal $d$-AlNiCo quasicrystal and find nonacoustic highly localized states at very low energies. Clearly further studies along this line are necessary.

---

*Email address: r.a.brand@uni-duisburg.de

[1] D. Shechtman, I. Blech, D. Gratias, and J.W. Cahn, Phys. Rev. Lett. **53**, 1951 (1984).

[2] P.A. Kalugin, A.Yu. Kitaev, and L.S. Levitov, J. Phys. (France) Lett. **46**, L601 (1985); P. Bak, Phys. Rev. Lett. **54**, 1517 (1985);

Phys. Rev. B **32**, 5764 (1986).

[3] J.P. Lu, T. Odagaki, and J.L. Birman, Phys. Rev. B **33**, 4809 (1986).

[4] T. Jannsen, in *Quasicrystalline Materials*, edited by C. Janot and J.M. Dubois (World Scientific, Singapore, 1988), p. 327.

[5] M. Quilichini and T. Janssen, Rev. Mod. Phys. **69**, 277 (1997).

[6] J. Hafner, J. Phys. C **14**, L287 (1981); Phys. Rev. B **27**, 678 (1983); J. Phys. C **16**, 5773 (1983); J. Non-Cryst. Solids **75**, 253 (1985).

[7] M. Krajčí and J. Hafner, J. Non-Cryst. Solids **192&193**, 338 (1995); J. Hafner, M. Krajčí, and M. Mihalkovič, Phys. Rev. Lett. **76**, 2738 (1996).

[8] M. de Boissieu, M. Boudard, R. Bellissent, M. Quilichini, B. Hennion, R. Currat, A.I. Goldman, and C. Janot, J. Phys.: Condens. Matter **5**, 4945 (1993).

[9] M. Boudard, M. de Boissieu, S. Kycia, A.I. Goldman, B. Hennion, R. Bellissent, M. Quilichini, R. Currat, and C. Janot, J. Phys.: Condens. Matter **7**, 7299 (1995).

[10] A.I. Goldman, C. Stassis, R. Bellissent, H. Moudden, N. Pyka, and F.W. Gayle, Phys. Rev. B **43**, 8763 (1991).

[11] A.I. Goldman, C. Stassis, M. de Boissieu, R. Currat, C. Janot, R. Bellissent, H. Moudden, and F.W. Gayle, Phys. Rev. B **45**, 10 280 (1992).

[12] M. Quilichini, G. Heger, B. Hennion, S. Lefebre, and A. Quivy, J. Phys. (Paris) **51**, 1785 (1990).

[13] M. Quilichini, B. Hennion, G. Heger, S. Lefebre, and A. Quivy, J. Phys. II **2**, 125 (1992).

[14] T. Klein, G. Pares, J.B. Suck, G. Fourcaudot, and F. Cyrot-Lackmann, J. Non-Cryst. Solids **153&154**, 562 (1993); J.B. Suck, *ibid.* **153&154**, 573 (1993); in *Phonons '89*, edited by S. Hunklinger, W. Ludwig, and G. Weiss (World Scientific, Singapore, 1990), p. 397; in *Quasicrystalline Materials*, edited by C. Janot and J.-M. Dubois (World Scientific, Singapore, 1988), p. 337; J.B. Suck and H.J. Güntherodt, *ibid.*, p. 573.

[15] G. Poussigue, C. Benoit, M. de Boussieu, and R. Currat, J. Phys.: Condens. Matter **6**, 659 (1994).

[16] J.-B. Suck, Mater. Sci. Eng. (to be published).

[17] J.-B. Suck and H. Rudin, in *Glassy Metals II*, Vol. 53 of Topics in Applied Physics, edited by H. Beck and H.-J. Güntherodt (Springer Verlag, Berlin, 1983) p. 217.

[18] R.A. Brand, G. Coddens, A.I. Chumakov, and Y. Calvayrac, Phys. Rev. B **59**, R14 145 (1999).

[19] M.A. Chernikov, A. Bernasconi, C. Beeli, A. Schilling, and H.R. Ott, Phys. Rev. B **48**, 3058 (1993); M.A. Chernikov, A. Bianchi, E. Felder, U. Gubler, and H.R. Ott, Europhys. Lett. **35**, 431 (1996).

[20] K. Wang, C. Scheidt, P. Garouche, and Y. Calvayrac, J. Phys. I **2**, 1553 (1992).

[21] J.C. Lasjaunias, Y. Calvayrac, and Hongshun Yang, J. Phys. I **7**, 959 (1997).

[22] Ch. Wälti, E. Felder, M.A. Chernikov, H.R. Ott, M. de Boissieu, and C. Janot, Phys. Rev. B **57**, 10 504 (1998).

[23] M.A. Chernikov, A. Bernasconi, C. Beeli, A. Schilling, and H.R. Ott, Phys. Rev. B **48**, 3058 (1993).

[24] J.C. Lasjaunias, A. Sulpice, N. Keller, J.J. Préjean, and M. de Boissieu, Phys. Rev. B **52**, 886 (1995).

[25] It must be emphasized that the extraction of a $T^3$-like term in the low-temperature specific heat of $i$-AlPdMn is quite questionable: the magnetic contribution which must be subtracted represents 98% of the total $C_p$ at 1.6 K: J.C. Lasjaunias (private communication).

[26] F. Bert, G. Bellessa, A. Quivy, and Y. Calvayrac, Phys. Rev. B **61**, 32 (2000).

[27] N. Vernier, G. Bellessa, B. Perrin, A. Zarembowitch, and M. de Boissieu, Europhys. Lett. **22**, 187 (1993).

[28] R. Sterzel, C. Hinkel, A. Haas, A. Langsdorf, G. Bruls, and W. Assmus, Europhys. Lett. **49**, 742 (2000).

[29] E.S.R. Gopal, *Specific Heats at Low Temperatures* (Plenum Press, New York, 1966); F.H. Herbstein, Adv. Phys. **10**, 313 (1961); A.A. Maradudin, E.W. Montroll, and G.H. Weiss, *Theory of Lattice Dynamics in the Harmonic Approximation*, Solid State Physics suppl. 4 (Academic Press, New York, 1963).

[30] R. Lübbers, H.F. Grünsteudel, A.I. Chumakov, and G. Wortmann, Science **287**, 1250 (2000).

[31] R.C. Zeller and R.O. Pohl, Phys. Rev. B **4**, 2029 (1971); J.C. Lasjaunias and R. Maynard, J. Non-Cryst. Solids **6**, 101 (1971); J.C. Lasjaunias, A. Ravex, and M. Vandorpe, Solid State Commun. **17**, 1045 (1975); J.C. Lasjaunias, A. Ravex, M. Vandorpe, and S. Hunklinger, *ibid.* **88**, 1023 (1993).

[32] P.W. Anderson, B.I. Halperin, and C.M. Varma, Philos. Mag. **25**, 1 (1972); W.A. Phillips, J. Low Temp. Phys. **7**, 351 (1972).

[33] H.R. Schober, C. Oligschleger, and B.B. Laird, J. Non-Cryst. Solids **156-158**, 965 (1993).

[34] V.G. Karpov, M.I. Klinger, and F.N. Ignat'ev, Zh. Éksp. Teor. Fiz. **84**, 760 (1983) [Sov. Phys. JETP **57**, 439 (1983)]; M.A. Il'in, V.G. Karpov, and D.A. Parshin, *ibid.* **92**, 291 (1987) [**65**, 165 (1987)].

[35] B.B. Laird and H.R. Schober, Phys. Rev. Lett. **66**, 636 (1991); H.R. Schober and C. Oligschleger, Phys. Rev. B **53**, 11 469 (1996); A. Pasquarello, *ibid.* **61**, 3951 (2000).

[36] M.A. Ramos, R. König, E. Gaganidze, and P. Esquinazi, Phys. Rev. B **61**, 1059 (2000); S.M. Nakhmanson and D.A. Drabold, *ibid.* **61**, 5376 (2000); J. Classen, T. Burkert, C. Enss, and S. Hunklinger, Phys. Rev. Lett. **84**, 2176 (2000).

[37] H.R. Schober and B.B. Laird, Phys. Rev. B **44**, 6746 (1991).

[38] U. Buchenau, Yu.M. Galperin, V.L. Gurevich, D.A. Parshin, M.A. Ramos, and H.R. Schober, Phys. Rev. B **46**, 2798 (1992).

[39] A. Katz and D. Gratias, in *Proceedings of the 5th International Conference on Quasicrystals*, edited by Ch. Janot and R. Mosseri (World Scientific, Singapore, 1995), pp. 164-167.

[40] M. Cornier-Quiquandon, A. Quivy, S. Lefebvre, E. Elkaim, G. Heger, A. Katz, and D. Gratias, Phys. Rev. B **44**, 2071 (1991); M. Quiquandon, A. Quivy, J. Devaud, F. Faudot, S. Lefebvre, M. Bessière, and Y. Calvayrac, J. Phys.: Condens. Matter **8**, 2487 (1996).

[41] D. Gratias, M. Quiquandon, and A. Katz, in Proceedings of the Spring School on Quasicrystals, Aussois, France, 1999, edited by E. Belin-Ferré, C. Berger, M. Quiquandon, and A. Sadoc (World Scientific, Singapore, in press).

[42] Y. Calvayrac, A. Quivy, M. Bessière, S. Lefebre, M. Cornier-Quiquandon, and D. Gratias, J. Phys. (France) **51**, 417 (1990).

[43] R.A. Brand, J. Voss, and Y. Calvayrac, in *Mössbauer Spectroscopy in Materials Science*, edited by M. Miglierini and D. Petridis (Kluwer Academic Publishers, Dordrecht, 1999), p. 299.

[44] G. Coddens, Int. J. Mod. Phys. B **11**, 1679 (1997).

[45] A.I. Chumakov and R. Rüffer, Hyperfine Interact. **113**, 59 (1998); A.I. Chumakov, Phys. Status Solidi B **215**, 165 (1999); A.I. Chumakov and W. Sturhahn, Hyperfine Interact. **123/124**, 781 (1999); W. Sturhahn and A.I. Chumakov, *ibid.* **123/124**, 809 (1999); W. Sturhahn, *ibid.* **125**, 149 (2000); V.G. Kohn and A.I. Chumakov, *ibid.* **125**, 205 (2000).

[46] M. Bée, *Quasielastic Neutron Scattering* (Adam Hilger, Bristol, 1988).

[47] See http://www.ill.fr/YellowBook/IN6/

[48] S.W. Lovesey, *Theory of Neutron Scattering from Condensed Matter* (Oxford, University Press, Oxford 1984), Vol. 1.

[49] A.J. Dianoux, Philos. Mag. **59**, 17 (1989).

[50] L.M. Needham, M. Cutroni, A.J. Dianoux, and H.M. Rosenberg, J. Phys.: Condens. Matter **5**, 637 (1993).

[51] F. Gompf, H. Lau, W. Reichert, and J. Salgado, in *Proceedings of the Conference on Neutron Inelastic Scattering* (I.A.E.A., Vienna, 1972), p. 137.

[52] P.A. Engelstaff and P. Schofield, Nucl. Sci. Eng. **12**, 260 (1962).

[53] R.A. Brand, J. Pelloth, F. Hippert, and Y. Calvayrac, J. Phys.: Condens. Matter **11**, 7523 (1999).

[54] R. Rüffer and A.I. Chumakov, Hyperfine Interact. **97/98**, 589 (1996).

[55] Neutron News **3**, 29 (1992).

[56] Program ''fitden5,'' ILL, was used. It includes up to five different bands of different atomic weight. See A. Fontana, F. Rocca, M.P. Fontana, B. Rossi, and A.J. Dianoux, Phys. Rev. B **41**, 3778 (1990).

[57] J.J. Vanderwal, P. Zhao, and D. Walton, Phys. Rev. B **46**, 501 (1992).

[58] W. Jones and N.H. Marsh, *Theoretical Solid State Physics* (Wiley-Interscience, New York, 1973), Chap. 3.

[59] A.I. Chumakov and W. Sturhahn, Hyperfine Interact. (to be published).

[60] J.C. Lasjaunias (private communication).

[61] J.J. Préjean, J.C. Lasjaunias, C. Berger, and A. Sulpice, Phys. Rev. B **61**, 9356 (2000).

[62] Y. Amazit, M. de Boissieu, and A. Zarembowitch, Europhys. Lett. **20**, 703 (1992).

[63] J. Dolinšek, B. Ambrosini, P. Vonlanthen, J.L. Gavilano, M.A. Chernikov, and H.R. Ott, Phys. Rev. Lett. **81**, 3671 (1998).

[64] G. Coddens, S. Lyonnard, B. Hennion, and Y. Calvayrac, Phys. Rev. Lett. **83**, 3226 (1999).

[65] W.-J. Zhu and C.L. Henley, Europhys. Lett. **46**, 748 (1999).

[66] M. Krajčí, J. Hafner, and M. Mihalkovič, Phys. Rev. B **62**, 243 (2000).